ISSN 1064-2269, Journal of Communications Technology and Electronics, 2017, Vol. 62, No. 9, pp. 976–983. © Pleiades Publishing, Inc., 2017.
Original Russian Text © Yu.A. Andreev, V.N. Kornienko, Sh. Liu, 2017, published in Radiotekhnika i Elektronika, 2017, Vol. 62, No. 9, pp. 882–889.

ANTENNA AND FEEDER SYSTEMS

Optimization of a Combined High-Power Ultrawideband Antenna

Yu. A. Andreev[a], *, V. N. Kornienko[b], and Sh. Liu[c]

[a] *Institute of High-Current Electronics, Siberian Branch, Russian Academy of Sciences, Tomsk, 634055 Russia*
[b] *Kotel'nikov Institute of Radio Engineering and Electronics, Russian Academy of Sciences, Moscow, 125009 Russia*
[c] *Shenyang Polytechnic University, Shenyang, 110159 People's Republic of China*
**e-mail: andreev@lhfe.hcei.tsc.ru*

Received May 26, 2016

Abstract—The results of optimization of the geometry of a combined ultrawideband antenna excited by a 1-ns bipolar pulse are presented. Numerical and physical experiments have been performed to optimize the increase in the electric-field strength in the direction of the antenna main beam. It has been shown that the peak field strength can be increased by 6%.

DOI: 10.1134/S1064226917080010

INTRODUCTION

High-power sources of ultrawideband (UWB) electromagnetic pulses have been actively investigated and developed for more than 20 years [1, 2]. One of the major problems in the development of high-power UWB sources is that of obtaining pulse electromagnetic fields with maximum possible peak amplitudes. The main parameter characterizing such sources is effective potential rE_p. It is defined as the product of peak electric-field strength E_p and far-zone distance r at which this field is measured.

Impulse radiation antennas (IRAs) [3], TEM antennas [4], and combined antennas (CAs) [5] are most frequently used as radiators in high-power sources of UWB radiation. Recently, sources with spiral antennas have also appeared [6, 7]. In this study, we consider optimization of CAs.

Combined antennas for radiation of high-power UWB pulses were proposed by Buyanov in the first half of the 1990s [2]. In the second half of the 1990s, he also proposed the idea of a CA with a widened passband, which was implemented in [5]. Characteristics of this CA were investigated in detail in [8]. Note that CAs are optimized for radiation of bipolar voltage pulses.

A series of high-power sources of UWB radiation with both a single transmitting antenna and an antenna array was developed at the Institute of High-Current Electronics, Siberian Branch, Russian Academy of Sciences. Generators of bipolar pulses with a duration of 0.2–3 ns and a pulse repetition rate of 100 Hz were used. The source of UWB radiation based on a 64-element CA array excited by a generator of bipolar voltage pulses with a duration of 1 ns, an amplitude of 200 kV, and a pulse repetition rate of 100 Hz [9] has the highest value of rE_p (4.3 MV). An element of this antenna array (whose design is close to that of antenna A1 from [8]) is used as a single radiator in a high-power source with an effective potential rE_p of 0.3 MV. It was a component of 16-element arrays with rE_p as high as 0.8 MV [10]. It is this CA that we will consider.

In [11], proposals for optimization of the CA aimed at an increase of E_p in the direction of the antenna main beam were made. These proposals were used in the development of modified CAs optimized for radiation of bipolar pulses with durations of 0.2 ns [12] and 2 ns [13]. However, in these studies, optimization was not aimed at increasing E_p in the direction of the main beam but at widening of the antenna passband. In [14], an antenna whose geometry was close to that of the CA was also optimized for widening of the passband.

In this study, we only consider optimization of the CA geometry aimed at increase in the peak amplitude of the electric-field strength E_p in the direction of the main beam of the directional pattern (DP).

1. GEOMETRY OF THE ANTENNA

The CA geometry is shown in Fig. 1. This antenna can be considered as a combination of an electric-type radiator made as a TEM horn with one active and two passive magnetic dipoles. The antenna input is a transition from a coaxial line to two strip lines. The lower strip line feeds the TEM horn, and the upper open-ended strip line, whose length is approximately h, feeds the active magnetic dipole.

As the object of investigation, we selected a CA with the length L = 16 cm, the height H = 15 cm

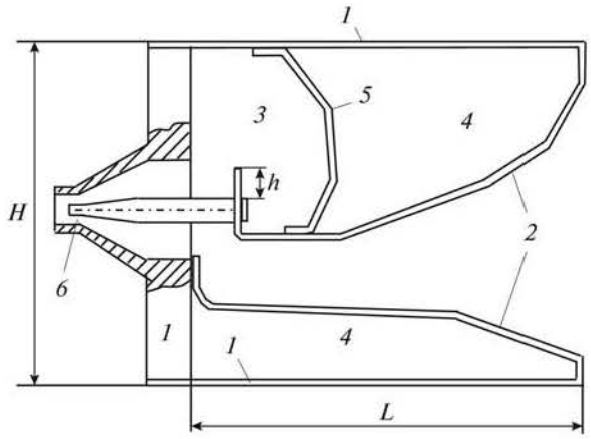

Fig. 1. Combined antenna: (*1*) housing, (*2*) TEM horn, (*3*) active magnetic dipole, (*4*) passive magnetic dipole, (*5*) additional electrode, and (*6*) N-type RF connector.

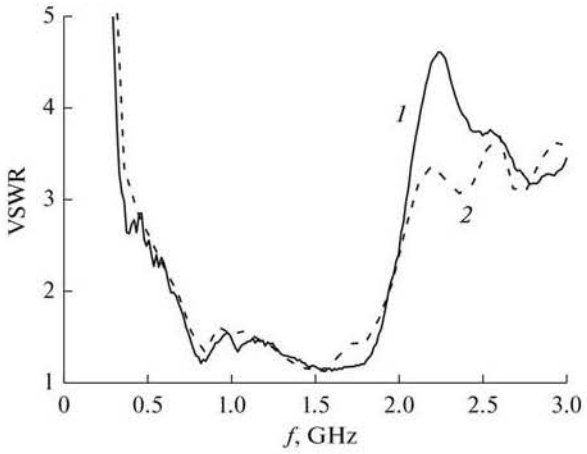

Fig. 2. VSWR of the CA obtained in the (*1*) actual and (*2*) numerical experiments.

(Fig. 1), and a width of 15 cm. The thickness of the aluminum plates used to construct the antenna (except for the back plate) is 1.7 mm.

Characteristics of this antenna were investigated in frequency and time domains.

2. NUMERICAL MODEL OF THE SYSTEM

For numerical simulation and calculation of the main characteristics of the antenna, we used a software system developed at the Kotel'nikov Institute of Radio Engineering and Electronics, Russian Academy of Sciences.

The system consists of three blocks; the data exchange between these blocks is performed with the use of long-term-storage files. The first block is used for calculation space–time dependences of all components of the electromagnetic field generated by the pulse source in the region that contains conducting and dielectric irregularly shaped 3D objects. This part of the system is based on a parallel algorithm for solution of nonstationary Maxwell equations using the finite difference grid method [15]. The linear dimensions of the region in which the solution is constructed are 15–20 wavelengths corresponding to the center frequency of the exciting pulse and several times larger than the maximum dimension of the antenna under consideration. The result of operation of the first block is time dependences of six field components at observation points located on the hemisphere centered at the point of intersection of the symmetry axis of the feeding coaxial line and the boundary of the region.

The second block uses these data to calculate the vector of the electric-field strength at a considerable distance from the antenna. The program of this part implements an algorithm based on retarded-time integral relations for field equations [16]. In this case, the integral relations can be used owing to the fact that the medium outside the antenna is homogeneous and isotropic and no reflections of the electromagnetic field occur outside the above-mentioned hemisphere.

The third part of the system uses the results obtained by the second block and makes it possible to calculate such antenna characteristics as the effective potential and DPs of various types.

3. FREQUENCY-DOMAIN AND TIME-DOMAIN CHARACTERISTICS OF THE COMBINED ANTENNA

To estimate the degree of agreement between the results of the numerical simulation and the actual experiment, the CA characteristics obtained in the respective cases were compared.

For investigation of the matching of the CA to the feeder line, the voltage standing-wave ratio (VSWR) was measured. The measurements were made on an Agilent N5227 microwave network analyzer with a frequency range of 67 GHz. The antenna radiation characteristics were measured in an anechoic chamber. The antennas were investigated in the radiation mode. Bipolar pulses with a duration of 1 ns and an amplitude of –45/+41 V were fed to the antenna input. To record the radiated pulses, we used a receiving antenna in the form of half a TEM horn since it introduces the minimum distortion into the time dependence of the electromagnetic field [17]. The pulses from the output of the receiving antenna were recorded by a LeCroy Wave Master 830Zi-A 30-GHz oscilloscope.

Figure 2 shows the antenna VSWR as a function of frequency.

Figure 3 shows calculated and experiment pulses radiated by the CA in the direction corresponding to $\varphi = 0°$, $\delta = 0°$, where φ is the azimuth angle and δ is

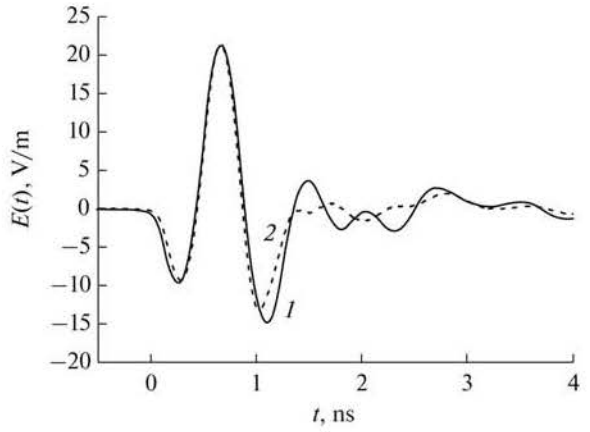

Fig. 3. Plots of the (*1*) experimental and (*2*) calculated oscillograms of the antenna radiation in the forward direction.

the angle of elevation. The pulse was recorded at a distance of 2.54 m from the transmitting antenna.

These plots show that the calculated and experimental data practically coincide during 1 ns. The maximum difference between the calculated and experimental data is observed in the after-pulse oscillations (at $t > 1.35$ ns), which can be explained by the difference between the actual CA feeder system and the ideal coaxial line whose model was used in the numerical calculation.

Figure 4 presents the calculated and measured H- and E-plane CA DPs normalized to the peak amplitude of the vertically polarized component of the field.

The data presented in Figs. 3 and 4 show that characteristics of the numerical model of the antenna are close to those of the actual CA. This fact makes it possible to use this model in the search for the optimum geometry.

4. POSSIBLE APPROACHES TO OPTIMIZATION OF THE COMBINED ANTENNA

Let us consider various methods for optimization of the CA under consideration. The first method is to improve matching of the antenna to the feeder in the maximum possible frequency range (without using absorbing materials) and thus increase the portion of the radiated energy.

Let us estimate the possible gain. Knowing the spectrum of the voltage pulse at the antenna input and the antenna VSWR, it is possible to find the energy contained in the generator pulse [7]

$$W_g = \int U_g^2(f)df \qquad (1)$$

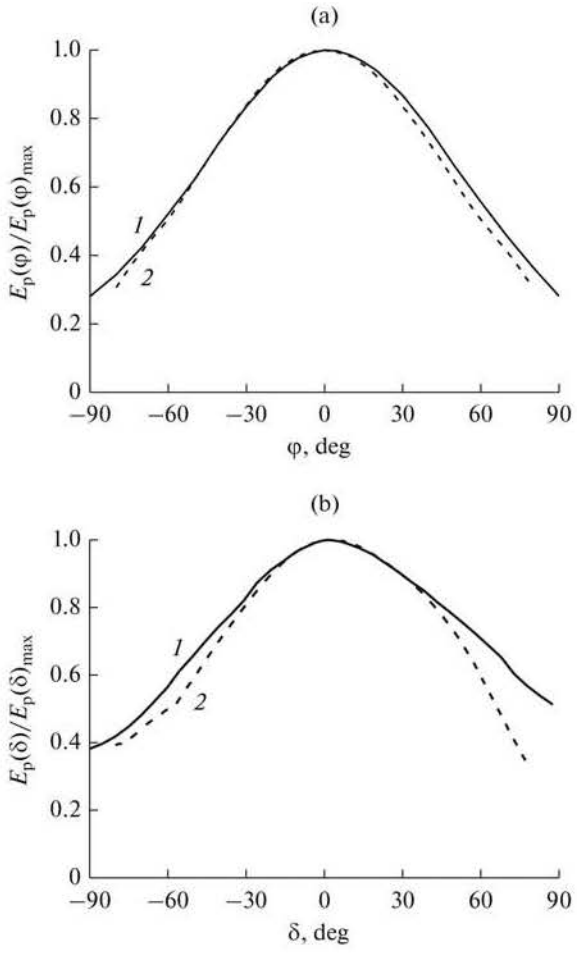

Fig. 4. Plots of (a) H- and (b) E-plane CA DPs normalized to the peak amplitude: (*1*) experiment and (*2*) calculation.

and the energy reflected from the CA [7]

$$W_{refl} = \int U_g^2(f)\left(\frac{K_V(f)-1}{K_V(f)+1}\right)^2 df, \qquad (2)$$

where $U_g(f)$ is the amplitude spectrum of the generator voltage pulse and K_V is the antenna VSWR.

Upon integrating power spectral density U_g^2 over the entire frequency range, we obtain the energy contained in the generator pulse. The maximum of the spectrum of the input bipolar voltage pulse corresponds to a frequency of 1 GHz. It can be seen in Fig. 2 that the antenna VSWR ≤ 1.5 in the frequency range from 0.75 to 1.875 GHz. Integrating the right-hand side of (1) over this frequency range, we find that it contains 65% of the energy of the incident pulse. Using (2), we can show that less than 4% of this energy is reflected from the antenna back into the feeder (VSWR ≤ 1.5). Thus, the antenna is already well

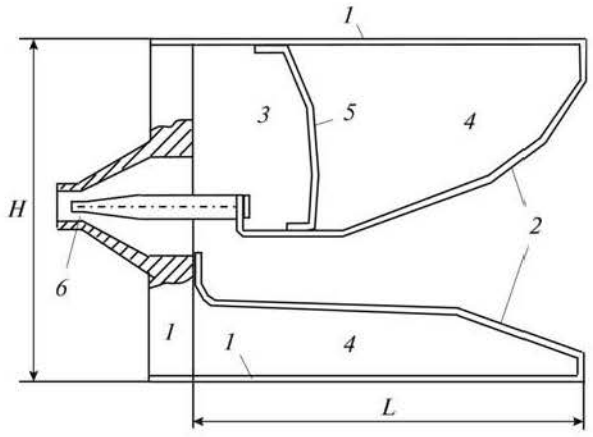

Fig. 5. Second modification of the CA: (*1*) housing, (*2*) TEM horn, (*3*) active magnetic dipole, (*4*) passive magnetic dipole, (*5*) additional electrode, and (*6*) N-type RF connector.

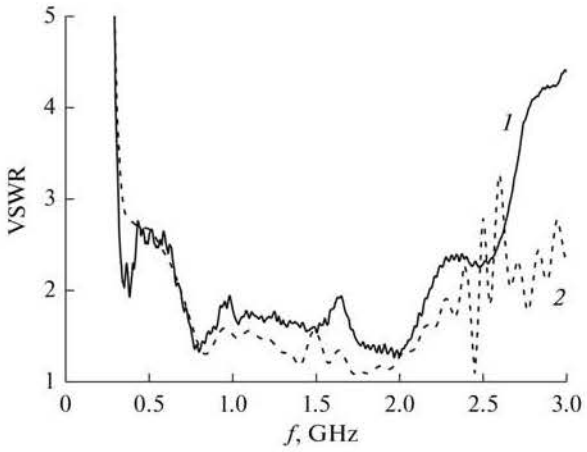

Fig. 6. VSWR of the second modification of the CA: (*1*) actual experiment and (*2*) numerical experiment.

matched in the given frequency range and it is very difficult to attain a significant decrease in the VSWR in this range. Even if the CA is perfectly matched in this frequency range (VSWR = 1), an increase in the radiated energy will be negligible.

The possibility of improvement of the antenna matching is related to the regions lower and upper frequencies. At upper frequencies ($f > 1.875$ GHz), it is possible to improve matching of the CA to the feeder circuit; however, no any significant increase in the energy radiated by the CA will be obtained since the portion of the energy in the generator pulse corresponding to these frequencies is small (2% in the range from 1.875 to 20 GHz). The portion of the energy of the generator pulse at frequencies $f < 0.75$ MHz is considerable (33%); however, it is extremely difficult to improve the antenna matching without increasing its dimensions and without introducing absorbing materials into its volume. Even if the VSWR is lowered in this frequency region and the portion of the radiated energy is increased, we will not be able to significantly increase E_p in the direction corresponding to $\varphi = 0°$, $\delta = 0°$, since the antenna DP is wide at lower frequencies and, therefore, the radiated energy is weakly focused.

The second method is to narrow down the antenna beam and increase the power flux density in the chosen direction. In this approach, the aperture of the transmitting antenna must usually be increased. In this study, it is assumed that, optimizing the CA geometry, we retain the antenna overall dimensions. Therefore, it is impossible to increase E_p in the direction of the main beam by increasing the antenna aperture and, therefore, by narrowing the DP.

The third method is to stabilize the position of the main beam in the maximum possible frequency range. This method can be interpreted as widening of the antenna bandwidth.

5. RESULTS OF OPTIMIZATION OF THE COMBINED ANTENNA

In [11], it was proposed to improve matching of the CA in the region of upper frequencies by decreasing height h of the coaxial-to-stripline transition. The first modification of this antenna with $h = 0$ was numerically investigated. Variation in height h does not affect matching of the antenna to the feeder in the region of lower frequencies. An insignificant increase in the VSWR (up to VSWR = 1.7) occurs in the region of medium frequencies, and a significant improvement is observed in the region of upper frequencies. Thus, the calculated upper boundary frequency corresponding to the VSWR = 1.5 shifted from $f = 1.825$ GHz to $f = 2.08$ GHz. The spatial distribution of the radiated field and the shape of the radiated pulse remained practically unchanged. Peak field amplitude E_p increased by 1.5%. This assumption was confirmed by the pulse investigations of the antenna. The measurement results show an increase in amplitude E_p of the modified antenna by 1%.

The second modification of the antenna is also presented in [11] (Fig. 5). In this modification, an attempt was made to improve the antenna matching in both lower- and higher-frequency regions. In this model, the height of the coaxial-to-stripline transition $h = 0$, the flare angle of the CA TEM horn is increased (by modifying the geometry of the upper surface of the TEM horn), and the geometry of additional electrode *5* (Fig. 1) is changed (its middle segment is shifted toward the back wall of the antenna by 1.5 cm. Figure 6 shows the antenna VSWR. It can be seen in the figure that the antenna matching in the physical

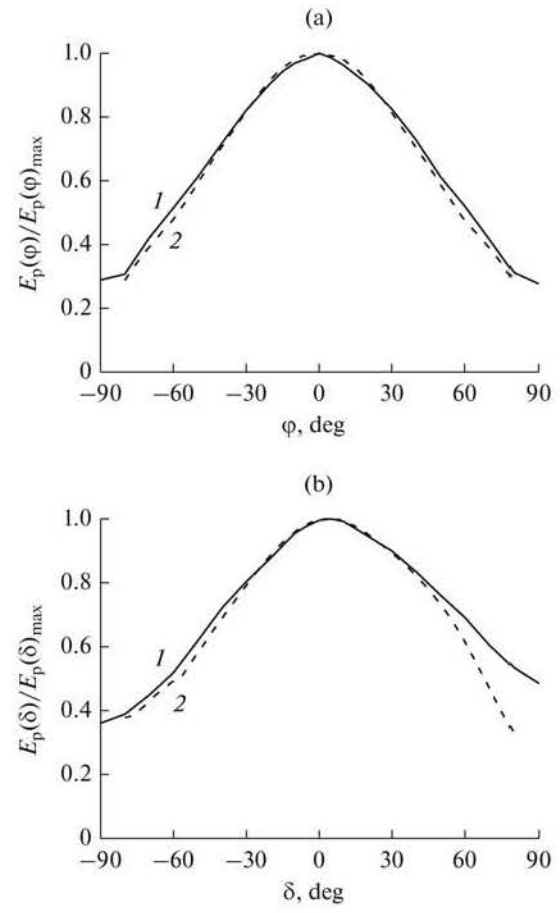

Fig. 7. Plots of (a) the H- and (b) E-plane DPs of the second modification of the CA normalized to the peak amplitude: (*1*) experiment and (*2*) calculation.

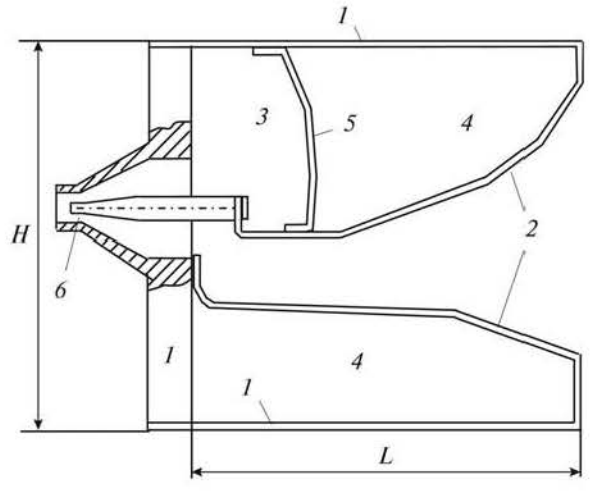

Fig. 8. Third modification of the CA: (*1*) housing, (*2*) TEM horn, (*3*) active magnetic dipole, (*4*) passive magnetic dipole, (*5*) additional electrode, and (*6*) N-type RF connector.

experiment is worse than in numerical one at the medium and upper frequencies, which is probably due to the difference in the geometries of the actual antenna and numerical model.

In this study, the spatial distribution of the field radiated by the antenna has been investigated. Figure 7 shows calculated and measured H- and E-plane DPs of the second modification of this antenna normalized to the peak field amplitude.

The shape of the radiated pulse remained practically the same. Peak field amplitude E_p increased by 3% in the numerical experiment and by 1.5% in the physical experiment.

6. RESULTS OF OPTIMIZATION OF THE COMBINED ANTENNA WITH AN INCREASED APERTURE

The above-mentioned modifications of the CA were based on the improvement of matching of the antenna to the feeder circuit in the maximum possible frequency range. The conducted investigations show that obtaining a considerable increase in the CA effective potential in the direction of the main beam without changing the antenna overall dimensions is a very difficult problem. Let us try to solve the problem of increasing antenna effective potential rE_p in the direction corresponding to $\varphi = 0°$, $\delta = 0°$ by stabilizing the position of the DP maximum over a wider frequency range. Here, it is logical to align the absolute maximum of the antenna DP with the desired direction of the rE_p maximum. Note that the maxima of the CA DP as well as maxima of DPs of its first and second modifications correspond to the direction $\varphi = 0°$, $\delta \cong 5°$ (Figs. 4b, 7b).

We will proceed from the fact that the antenna DP is symmetrical with respect to the horizontal plane if the antenna itself is symmetrical with respect to this plane. This (third) modification of the CA is presented in Fig. 8. The third modification differs from the second one in that height H is increased by 3 cm (H = 18 cm) due to the increase in the dimensions of the lower passive magnetic dipole (Fig. 8, element *4*). Therefore, the third modification of the CA is based on an increase in the aperture of the transmitting antenna.

Figure 9 shows the VSWR of the third modification of the CA. It can be seen from the figure that, in the upper-frequency region, the antenna matching in the physical experiment is considerably worse than in the numerical experiment. This disagreement is probably due to the difference between the geometries of the actual antenna and of the numerical model. However, since this disagreement is observed at frequencies $f \geq 2$ GHz, it should not significantly affect the value of rE_p.

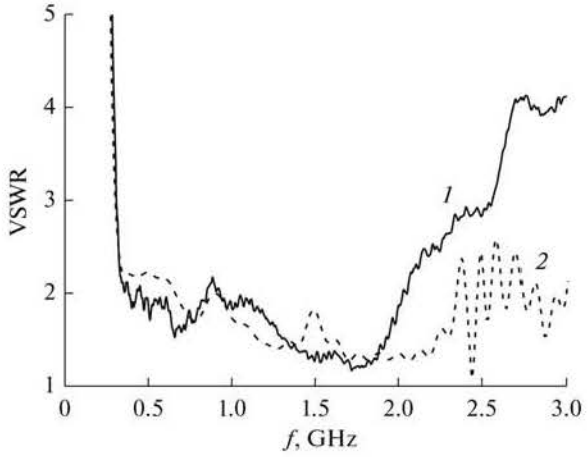

Fig. 9. VSWR of the third modification of the CA: (*1*) actual experiment and (*2*) numerical experiment.

Figure 10 shows calculated and measured H- and E-plane DPs of the third modification of the CA normalized to the peak field amplitude.

The calculated and measured 0.707-level beamwidths of the CA and its modifications are given in the Table 1.

The data listed in the Table 1 show that the main-beam width of the second and third modifications of the CA only slightly decreasesin the H plane and considerably decreases in the E plane. The DP maximum in the E plane for the the third modification of the CA corresponds to the elevation angle $\delta \cong 0°$.

As compared to the base version, peak field amplitude E_p produced by the third modification of the CA increased by 6.5% in both the numerical and actual experiments.

Note that we selected the third modification of the antenna geometry (with antenna height H increased by 3 cm) taking into consideration the geometry of the high-power UWB-pulse source, which is based on a 64-element CA array [9], with an aim of probable modification of this source. However, it is clear that the CA can be optimized without increasing height H. In this case, the CA input is shifted upward with simultaneous symmetrization of the TEM horn. In this case, the increase in rE_p will be less than 6.5% but the radiation maximum of the compact CA will correspond to $\varphi = 0°$, $\delta = 0°$ and the E-plane DP will be more symmetric.

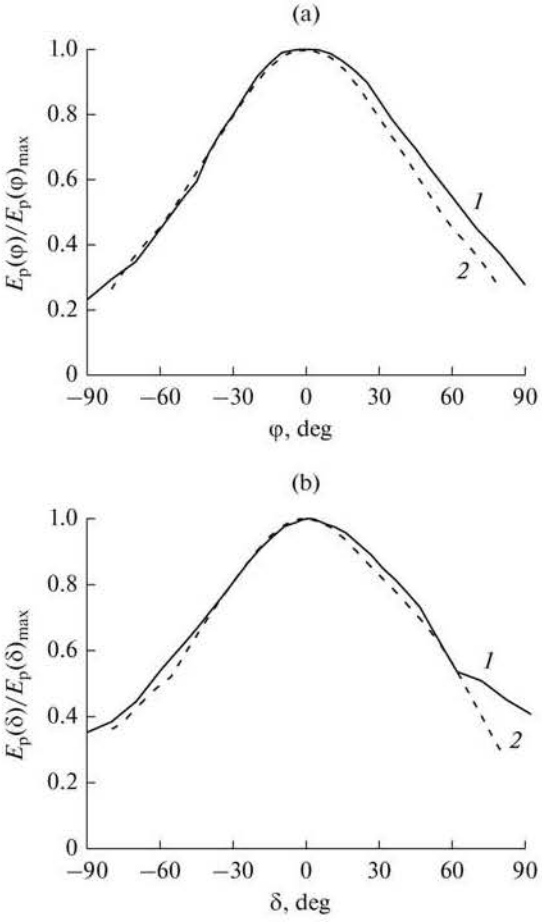

Fig. 10. Plots of (a) the H- and (b) E-plane DPs of the third modification of the CA normalized to the peak amplitude: (*1*) experiment and (*2*) calculation.

Amplitude–frequency and phase–frequency characteristics (AFCs and PFCs, respectively) of the CA and its second and third modifications were measured. The investigations were conducted in an anechoic

Table 1. Widths of the main beam for the CA and its modifications

CA type	Calculation		Experiment	
	H plane	E plane	H plane	E plane
Initial CA	84.5°	93°	88°	106°
Second modification	80°	91°	83°	100°
Third modification	75°	83°	81°	87°

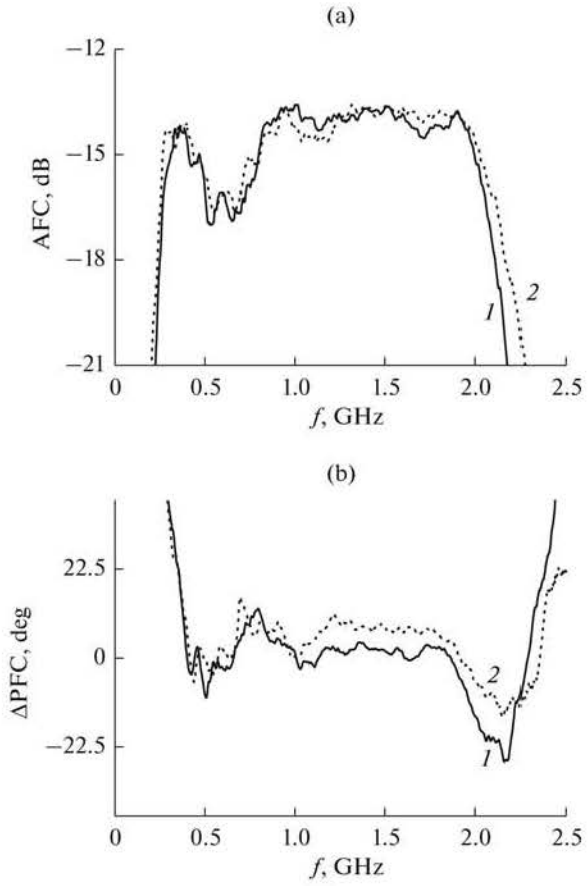

Fig. 11. Plots of the (a) AFCs and (b) deviations from the linear PFCs for the (*1*) CA and (*2*) its third modification.

chamber with the use of an Agilent N87189ET microwave network analyzer. We will define the passband of the antenna as the frequency range in which the conditions for low-distortion signal transmission are satisfied, namely: variations in the antenna AFC with respect to the mean value are within ±1.5 dB and the deviation of the PFC from a linear function are within $\pm\pi/16$ [8]. Figure 11 shows the AFCs and the deviations from the linear PFC for the CA and its third modification.

The passband lower boundary frequency f_l is determined by the deviation of the PFC from a linear function. For the CA and its modifications, $f_l \cong 0.38$ GHz. The passband upper boundary frequency f_u is determined by the deviation of the PFC from a linear function or deviation of the AFC from the mean value by 1.5 dB. The CA passband is 5.2, and it increases up to 5.7 for the second modification. The passband of the third modification of the CA is 5.6, which is probably due to the inaccuracies of the antenna manufacturing process. Widening of the CA passband makes it possible to not only obtain higher effective potential rE_p when the antenna is excited by a bipolar pulse but also efficiently radiate UBPs of a shorter duration or a different shape.

CONCLUSIONS

In the numerical and actual experiments, the CA and its various modifications have been investigated. The CA excited by a 1-ns bipolar voltage pulse has exhibited high efficiency in generation of effective potential rE_p in the direction corresponding to $\varphi = 0°$, $\delta = 0°$. It has been shown that the CA passband $f_u/f_l = 5.2$ can be expanded up to 5.7 (for the second modification) in the direction corresponding to $\varphi = 0°$, $\delta = 0°$ without changing the antenna overall dimensions. In this case, rE_p increases by 3% in the numerical experiment and by 1.5% in the real experiment.

A modification of the CA (the third modification) with increased height H has been proposed. This modification also has an expanded passband ($f_u/f_l = 5.6$) and its effective potential is increased by 6.5%. These antennas with a height-to-width ratio of 1.2 can be promising elements of CA arrays. The maximum of the DP of the third modification of the CA corresponds to the direction $\varphi = 0°$, $\delta = 0°$, and the E-plane DP itself is more symmetric with respect to the horizontal plane.

ACKNOWLEDGMENTS

We are grateful to the Tomsk Center for Collective Use of Equipment, Siberian Branch, Russian Academy of Sciences, for providing the LeCroy Wave Master 830Zi-A and Agilent N5227A instruments. Numerical simulation was performed with the computational resources of the Interdepartamental Supercomputer Center, Russian Academy of Sciences.

REFERENCES

1. C. E. Baum and E. G. Farr, *Ultra-Wideband, Short-Pulse Electromagnetics* (Plenum, New York, 1993).
2. V. I. Koshelev, Yu. I. Buyanov, B. M. Kovalchuk, et al., Proc. SPIE **3158**, 209 (1997).
3. D. V. Giri, H. Lackner, I. D. Smith, et al., IEEE Trans. Plasma Sci. **25**, 318 (1997).
4. P. Delmote and B. Martin, *Ultra-Wideband, Short-Pulse Electromagnetics 9* (Springer, New York, 2010), p. 315.
5. V. I. Koshelev, Yu. I. Buyanov, Yu. A. Andreev, et al., in *Proc. 28th IEEE Conf. Plasma Sci. & 13th IEEE Int. Pulsed Power Conf. Las Vegas, Nevada, USA, June 17–22, 2001* (New York, IEEE, 2001), Vol. 2, p. 1661.
6. D. Morton, J. Banister, T. Da Silva, et al., in *Proc. 2010 IEEE Int. Power Modulator and High Voltage Conf., Atlanta, May 23–27, 2010* (IEEE, New York, 2010), p. 186.

7. Yu. A. Andreev, A. M. Efremov, V. I. Koshelev, et al., Rev. Sci. Instrum. **85**, 104703 (2014).
8. Yu. A. Andreev, Yu. I. Buyanov, and V. I. Koshelev, J. Commun. Technol. Electron. **50**, 535 (2005).
9. A. M. Efremov, V. I. Koshelev, B. M. Kovalchuk, et al., Laser Particle Beams **32**, 413 (2014).
10. A. M. Efremov, V. I. Koshelev, B. M. Koval'chuk, V. V. Plisko, and K. N. Sukhushin, J. Commun. Technol. Electron. **52**, 756 (2007).
11. Yu. A. Andreev and S. Liu, in *Proc. 15th Int. Symp. on High Current Electronics, Tomsk, Sep. 21–26, 2008* (IHCE, Tomsk, 2008), p. 387.
12. Yu. A. Andreev, A. M. Efremov, V. I. Koshelev, et al., in *Proc. 15th Int. Symp. on High Current Electronics, Tomsk, Sep. 21–26, 2008* (IHCE, Tomsk, 2008), p. 447.
13. Yu. A. Andreev, V. I. Koshelev, I. V. Romanchenko, V. V. Rostov, and K. N. Sukhushin, J. Commun. Technol. Electron. **58**, 297 (2013).
14. A. Mehrdadian and K. Forooraghi, Progress Electromagn. Res. C **39**, 37 (2013).
15. V. N. Kornienko and V. A. Cherepenin, J. Commun. Technol. Electron. **48**, 691 (2003).
16. *Computer Techniques for Electromagnetics*, Ed. by R. Mittra (Pergamon, Oxford, UK, 1973; Mir, Moscow, 1977).
17. Yu. A. Andreev, V. I. Koshelev, and V. V. Plisko, *Radar and Radio Communication (Proc. 3rd All-Rusia Sci.-Techn. Conf., Moscow, Nov. 21–26, 2011)* (Kotel'nikov IRE RAN, Moscow, 2011), p. 77.

Translated by I. Nikishin